RSC Advances

This article can be cited before page numbers have been issued, to do this please use: P. arora, J. K. Rajput and H. Singh, *RSC Adv.*, 2015, DOI: 10.1039/C5RA20150K.

ROYAL SOCIETY OF CHEMISTRY

www.rsc.org/advances

View Article Online
DOI: 10.1039/C5RA20150K

Nanostructured Oxytyramine Catalyst for Peerless One-Pot Synthesis of Cyclohexanecarbonitrile Derivatives

Priya Arora, Jaspreet Kaur Rajput[#], Harminder Singh

Department of Chemistry, Dr. B R Ambedkar National Institute of Technology, Jalandhar -144011, Punjab, India

Corresponding Author: [#]rajputj@nitj.ac.in, Tel.: +91-181-2690301 02x2208; fax: +91 181 2690320

Abstract

Magnetic recyclable heterogeneous organocatalyst OT@Si@SPIONs, has been developed in this report, with the aim to synthesize cyclohexanecarbonitriles. The prepared nanocatalyst was fully characterized with various techniques and its catalytic activity has been checked by one pot reaction which involves in situ formation of imine from cyclohexanone and amines which further undergo nucleophilic addition with TMSCN. Moreover, although this Strecker reaction is century old reaction, its applicability with ketones is still a less explored subject, and our investigation provided an insight into the efficient synthesis of cyclohexanecarbonitrile derivatives using a ketone i.e. cyclohexanone. As compared with other reported catalytic systems in literature our showed superior catalytic activity at a remarkably low catalyst loading i.e. 5 mg.

Keywords: *Oxytyramine* anchored Si-SPIONs, magnetically recoverable heterogeneous catalyst, cyclohexanecarbonitrile derivatives, green, recyclable.

1. Introduction

Combination of nanotechnology with green chemistry had proven to be a boon for industries [1]. Chemical and pharmaceutical industries are keenly looking forward for economical and environmentally benign measures of recycling catalyst [2] as homogeneous catalysis though endowed with chemo, regio and enantioselectivity of the catalyst imposes difficulty of catalyst separation from the final product [3]. In such respect, nano-magnetic catalysis plays a major role in heterogeneous catalysis as it provides easy magnetic recovery of catalyst from the reaction mixture with the help of a permanent magnet [4] hence vanishing the use of conventional techniques like filtration and centrifugation etc. Nanocatalysts either metallic nanoparticles or supported magnetic nanoparticles have high catalytic activity, high degree of chemical stability, act as simple, robust, readily available high surface area heterogeneous catalysts [5]. Among the different magnetic nanocatalysts known to date, Fe_3O_4 nanoparticles have greatest impact in this field as they can efficaciously reinforce the functioning of different moieties by acting as a support to them [6] and result in heterogeneous and magnetically separable catalysts due to their superparamagnetic character. Albeit bare iron oxide nanoparticles are hard to handle due to their extreme reactive nature towards oxidation but this extreme reactivity can be mitigated by tailoring the surface of nanoparticles. Along with high

View Article Online
DOI: 10.1039/C5RA20150K

reactivity, many other pitfalls of bare nanoparticles like formation of large aggregates to minimize surface energies, loss of dispersibility, low thermal stability and high chemical activity can also be lessened by applying some protection strategies which include grafting or coating of an inert material [7]. The most studied inert material for protecting iron oxide nanoparticles is silica, which can be further used to anchor the catalytic molecules into its pores to generate catalytic centres [8]. Many organic ligands have also been reported to stabilize the magnetic nanoparticles and also for their particular application [9]. Magnetic iron nanoparticles and their functionalized counterparts have numerous applications in various fields such as data storage [10], catalysis [6,11], drug-targeting [12], cancer therapy [13], lymph node imaging or hyperthermia [14], magnetic resonance imaging [15], sensors [16] and many more.

Ample attention on bifunctional entities has been attracted in organic synthesis because of their vast applications in drug designing. Amino nitriles are potent representators of bifunctional compounds. Both amino and nitrile moieties can easily undergo diversity of modifications allowing rapid advance towards synthetically important organic products. Transformation of nitrile group in α-aminonitriles to carboxylic acid by hydrolysis leads to formation of α-amino acid and this transformation was first carried out by Adolph Strecker in 1850[17], thereafter termed as Strecker synthesis, since then vast research has been carried out on this reaction with various catalysts like $Yb(OTf)_3$-pybox[18], lanthanum(III)-binaphthyl disulfonate[19], Jacobsen's thiourea catalyst[20], mesoporous aluminosilicate (Al-MCM-41)[21], $Fe(Cp)_2PF_6$[22], N-heterocyclic carbene (NHC)-amidate palladium (II) complex[23], BINOL-phosphoric acid[24], K_2PdCl_4[25], gallium (III) triflate[26], IBX/TBAB[27], nanocrystalline magnesium oxide[28], superparamagnetic iron oxide[29] and Lewis base[30] e.g. N,N-dimethylcyclohexylamine etc., various sources of amino and cyano groups like HCN, KCN, $(EtO)_2P(O)CN$, Et_2AlCN, Bu_3SnCN and TMSCN[31,32]. Strecker reaction is the simplest and economical method for the synthesis of α-aminonitriles which are versatile synthons of various amino acids and many other bioactive compounds including natural products. Recently various pharmacologically useful compounds like phthalascidin 622[33], hepatitis C virus NS3 serine protease inhibitors[34] and boron containing retinoids[35] have been synthesized following this strategy. Strecker reaction with ketones has been rarely studied due to very slow reaction rates as ketones are challenging substrates due to their steric demands during the formation of C-C bond[36]. Often ketone Strecker reaction is carried out stepwise by using premade imines or by using high pressure conditions. Although some of one pot procedures have been reported but most of them involve the use of expensive reagents, harsh conditions, tedious work up and long reaction times. So we herein report the Strecker reaction involving ketones i.e. cyclohexanone as substrate with good results at ambient temperature and solvent free conditions. The advantage of this methodology is the simplicity of the procedure, which avoided the use of tedious chromatographic purification of products and no use of harsh organic solvents thus supporting the central issue of today's research i.e. green chemistry.

So in continuation of our previous work [37,38], we describe here environmentally sound protocol for facile synthesis of cyclohexanecarbonitrile derivatives using cyclohexanone. Herein, we also report

View Article Online
DOI: 10.1039/C5RA20150K

the preparation and structural determination of a new organocatalyst *oxytyramine* immobilized silica@Fe_3O_4 nanocatalyst. Oxytyramine is a naturally occurring catecholamine which acts as an inotropic agent. It is an essential part of human body as it has many important functions like it controls the motor abilities, motivation, concentration, sleep, mood, memory and learning etc [39]. It can improve the functioning of the heart and is also used for the treatment of Parkinson's disease. So the *oxytyramine* anchored Si-SPIONs can be used in variety of applications. The utilization of magnetic nanoparticles as catalysts for this reaction is one approach i.e. green, inexpensive, facile and widely applicable.

2. Result and Discussion

2.1 Synthesis of OT-Si-SPIONs

The core of the *oxytyramine* grafted-silica coated superparamagnetic iron oxide nanoparticles (OT-Si-SPIONs) has been synthesized by co-precipitation [40] method combined with low power sonication. Modified Stöber method [41] in addition to ultrasonication, has been used to prepare OT-Si-SPIONs, which has an advantageous effect that this method does not require any high temperature treatment to get crystalline nanoparticles as ultrasonic waves generate some localized hot spots which induce in situ calcinations [42]. *Oxytyramine* moiety has been coated on Si-SPIONs as former is high affinity binding molecule and thus stabilize the SPIONs. The $-NH_2$ group on the moiety could be used as the reaction site. The synthesis of magnetite nanoparticles and its functionalization have been represented in Scheme I.

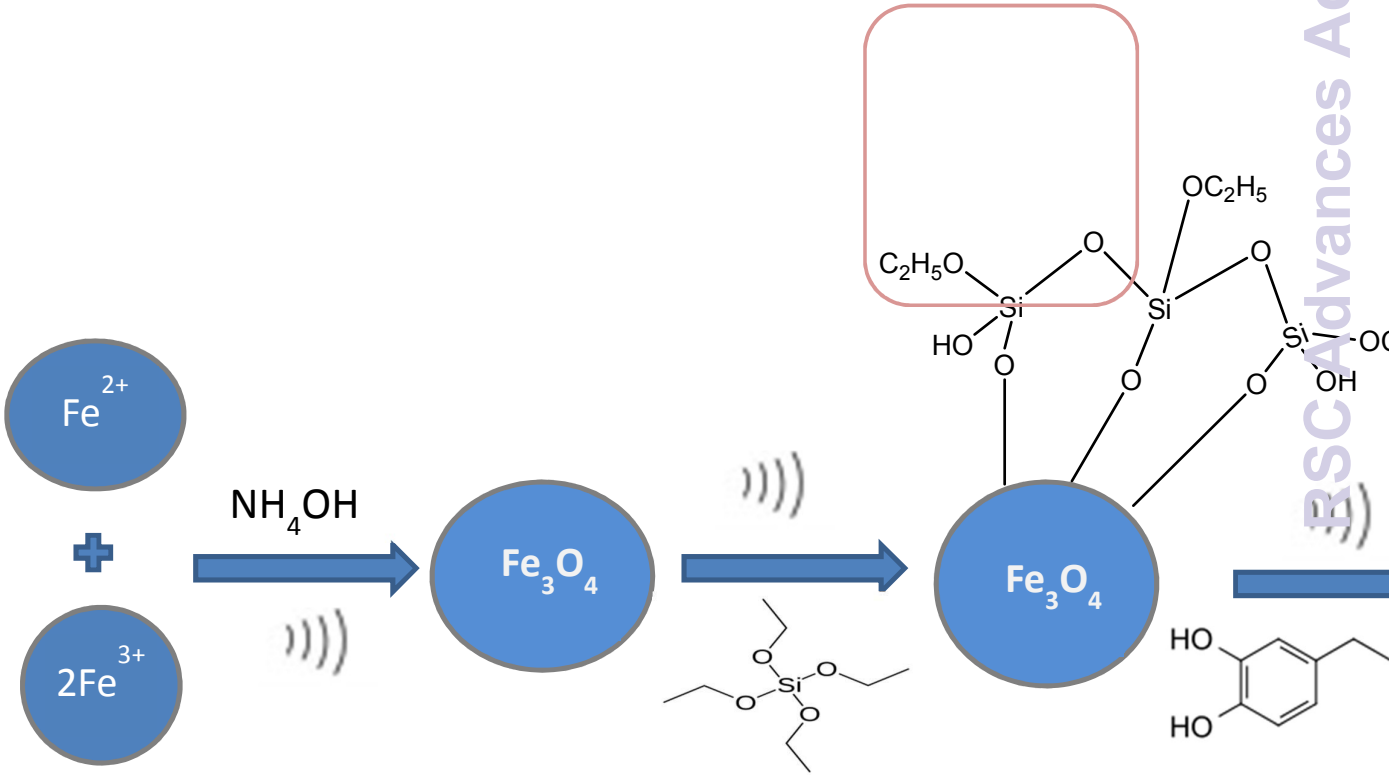

View Article Online
DOI: 10.1039/C5RA20150K

Scheme I: Schematic representation of coating of silica and *oxytyramine* over magnetite nanoparticles.

2.2 Characterization of prepared OT-Si-SPIONs

FT-IR:-

In order to depict the surface modification of SPIONs with TEOS and *oxytyramine*, the FT-IR spectra of SPIONs, Si-SPIONs and OT-Si-SPIONs are illustrated in Fig. 1A in which Fig. 1(a) displays FT-IR spectrum of SPIONs. The absorbance bands at 590 and 633 cm^{-1} are ascribed to Fe-O vibration and are consistent with the reported IR spectrum for spinel Fe_3O_4 [43]. The IR bands at 3393 and 1625 cm^{-1} are due to stretching and deformation vibration of –OH groups which are due to adsorbed water on the surface of magnetite nanoparticles. FT-IR spectrum of Si-SPIONs is shown in Fig. 1(b). The absorption band at 1097 cm^{-1} characteristic of Si-O group, demonstrate covalent bond between nanoparticles surface and silane. Bands at 957 cm^{-1} and 801 cm^{-1} are due to vibration of Si-O-Si groups. These results indicate successful immobilization of SiO_2 on the surface of Fe_3O_4 nanoparticles. Fig. 1(c) depicts the FT-IR spectrum of prepared OT-Si-SPIONs. Several new peaks at 1281, 1488 and 1614 cm^{-1}, characteristic of C-O vibrations, benzene ring C-C vibrations and N-H stretching respectively, confirms the successful coating of *oxytyramine* over silica coated magnetite nanoparticles.

XRD:-

As presented in Fig. 1B, SPIONs show characteristic diffraction peaks at different values of 2θ i.e. 30.12, 35.54, 43.13, 53.56, 57.17, 62.78 with corresponding diffraction planes 220, 311, 400, 422, 511 and 440 which are totally consistent with spinel cubic Fe_3O_4 diffraction peaks (JCPDS 19-0629) [44]. Fig. 1B(b) shows the XRD pattern of Si-SPIONs, showing exactly the same peaks as that of Fe_3O_4 nanoparticles in addition to it a broad hump at 2θ= 20-25º is observed which is characteristic of amorphous silica. The repetition of the same peaks depict that the crystallinity of the nanoparticles has been restored even after its functionalization. The XRD pattern of OT-Si-SPIONs is shown in Fig. 1B (c). The broad peak at 2θ= 20-25º in Si-SPIONs has been shifted to lower values due to synergistic effect of amorphous silica. Also the intensity of the characteristic peaks of SPIONs further decreases because of surface coating of shell layers, which confirms the cover-up of subsequent layers. The average size of SPIONs, as calculated by Debye Scherrer formula is found to be ~13 nm.

View Article Online
DOI: 10.1039/C5RA20150K

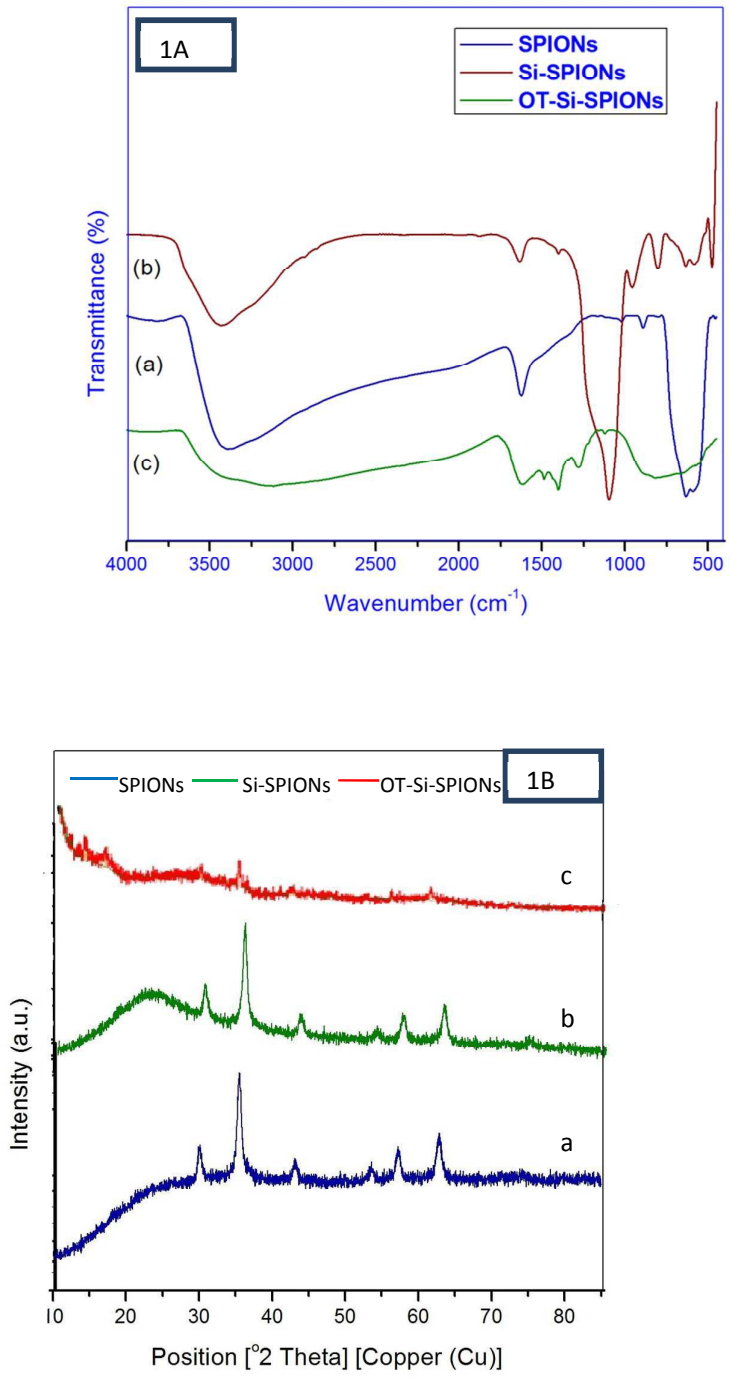

Fig. 1: A. FT-IR spectra of : (a) SPIONs; (b) Si-SPIONs; (c) OT-Si-SPIONs, B. XRD Spectra of: (a) SPIONs; (b) Si-SPIONs; (c) OT-Si-SPIONs.

Morphology:-

Fig. 2 displays the TEM (a-c) images of SPIONs, Si-SPIONs and OT-Si-SPIONs which reveal that iron oxide nanoparticles are spherical in nature with size ranging from 12-15 nm which is consistent with the size calculated from XRD data and are present in non-aggregate form. Fig. 2b shows the

View Article Online
DOI: 10.1039/C5RA20150K

core-shell structure of silica coated iron oxide nanoparticles and Fig. 2c portray the mosaic type structure of OT-Si-SPIONs in which organic moiety, *oxytyramine* has been coated over multiple Si-SPIONs. Fig. 2e shows the SEM image of OT-Si-SPIONs confirming its spherical shape.

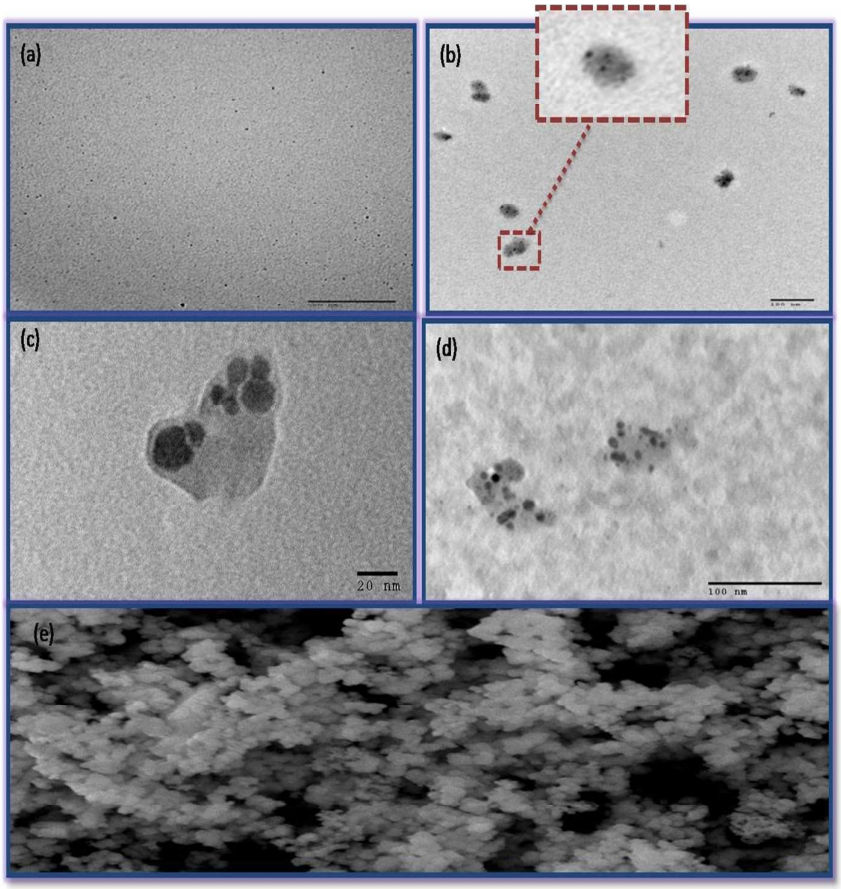

Fig. 2 TEM images of: (a) SPIONs; (b) Si-SPIONs; inset shows its core-shell structure (c) OT-Si-SPIONs; (d) Recovered OT-Si-SPIONs after 5th cycle; (e) SEM image of OT-Si-SPIONs.

Magnetic Properties:-

Vibrating sample magnetometer was used to examine the magnetic properties of synthesized nanoparticles i.e. OT-Si-SPIONs at room temperature. Fig. 3 describes the VSM plot of *oxytyramine* anchored Si-SPIONs, which depicts superparamagnetic nature of nanoparticles in which the saturation magnetization value comes out to be 2.413 emu/g which is very small as compared to its bulk value of uncoated SPIONs i.e. approximately 90 emu/g [45]. This decrease in saturation magnetization is because of very small size of the synthesized nanoparticles as there is a linear correlation between particle size and saturation magnetization and also due to non-magnetic layer on the surface of nanoparticles the value further decreases. The zero coercivity and small remanence value also proves the superparamagnetic properties of synthesized functionalized nanoparticles.

View Article Online
DOI: 10.1039/C5RA20150K

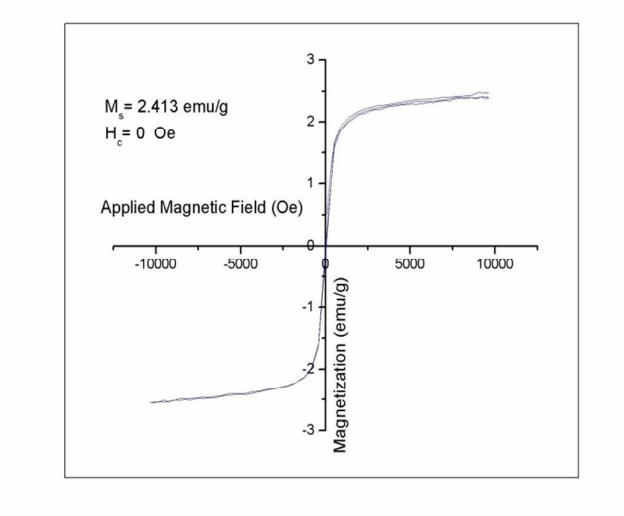

Fig. 3 VSM image of OT-Si-SPIONs.

Surface properties:-

Fig. 4 shows the N_2 adsorption-desorption isotherm of the OT-Si-SPIONs. The BET surface area of the particles was found to be 5.9115m^2/g, as calculated by linear part of the BET plot. The total pore volume at P/P_0 = 0.98 is 0.0106 cm^3/g and average pore diameter is 26.00626 nm. This pore size depicts the particles are mesoporous in nature [46]. The BET isotherm is of Type IV characteristic of porous material with pore size in the range of 1.5-100 nm [47].

View Article Online
DOI: 10.1039/C5RA20150K

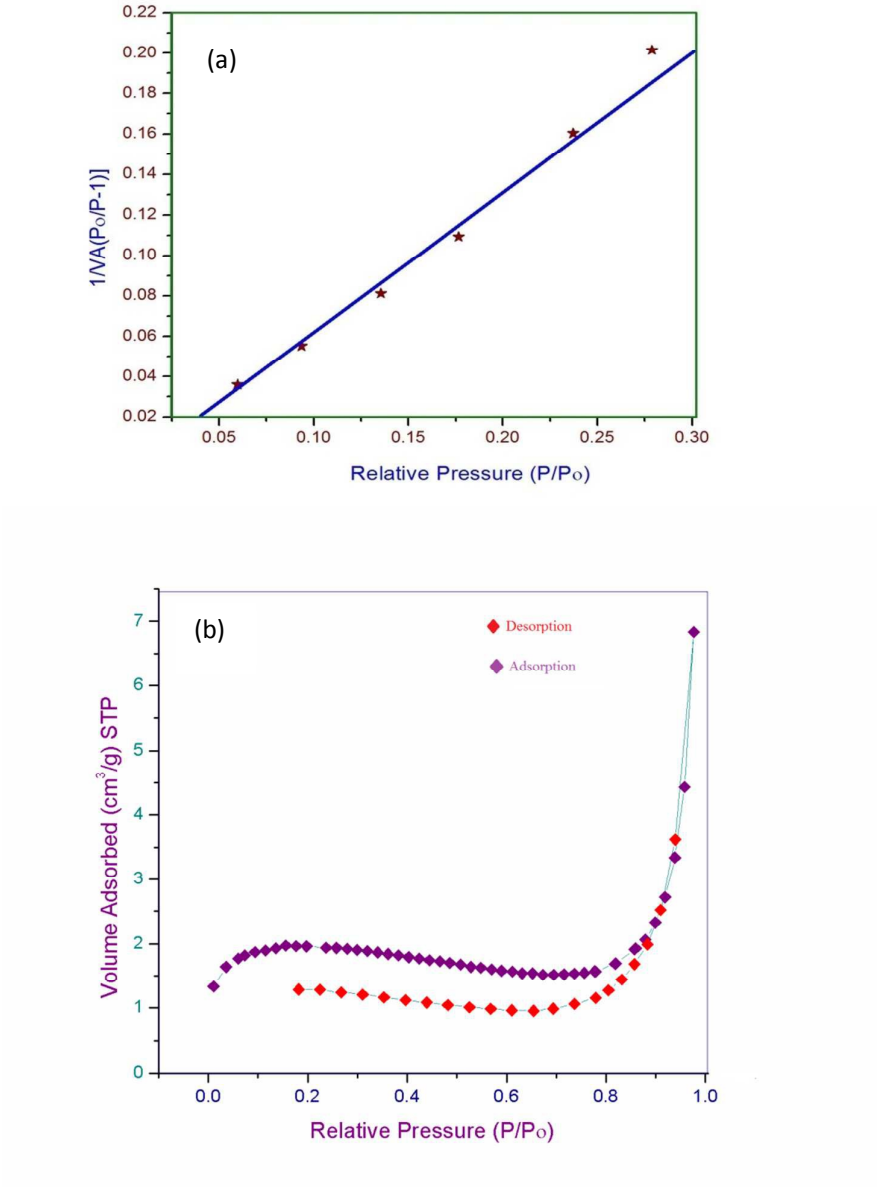

Fig. 4: (a) BET plot of OT-Si-SPIONs; (b) Type IV isotherm plot of OT-Si-SPIONs.

UV-Vis :-

UV-Vis spectral analysis (Fig. 5) has been used to confirm the formation and stability of magnetic nanoparticles in an ethanolic colloidal solution. Pure Fe_3O_4 nanoparticles absorbed light with wavelengths mainly below 750 nm (Fig. 5a), in comparison to Fe_3O_4 nanoparticles shift of absorption band towards lower wavelength i.e. blue shift was noticed on silica as well as *oxytyramine* coating over Fe_3O_4 nanoparticles. The UV-Vis spectra of the synthesized nanoparticles were also observed after 10 days, showing no significant change in the absorption peaks which confirms the stability of nanocatalysts.

View Article Online
DOI: 10.1039/C5RA20150K

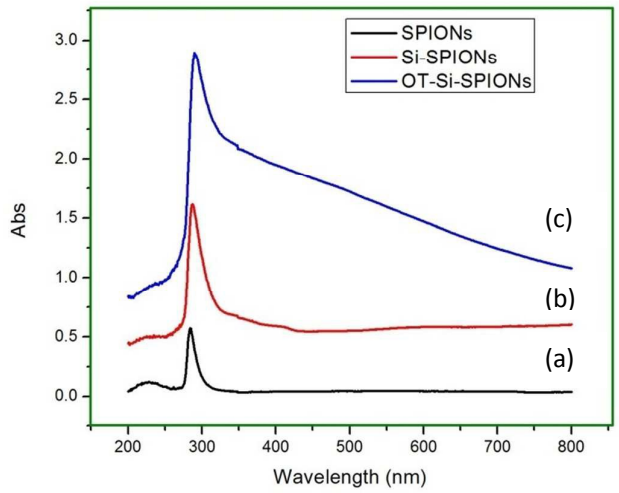

Fig. 5 UV-Vis spectra of: (a) SPIONs; (b) Si-SPIONs; (c) OT-Si-SPIONs.

TGA :-

To investigate the stability of the synthesized nanoparticles, thermo gravimetric analysis of SPIONs, Si-SPIONs and OT-Si-SPIONs has been performed from 40-750 °C at a heating rate of 10 °C/min under nitrogen atmosphere as shown in Fig. 6. In case of SPIONs initial weight loss of 1.9 % was observed in the temperature range of 100-350 ºC due to loss of moisture and after 350 °C only 0.9 % weight loss was seen till 700 °C. In case of Si-SPIONs, two stages of weight loss are observed in the temperature range of 40-100°C and 100-600°C. The initial weight loss of 3.8 % at first stage corresponds to loss of adsorbed water and ethanol. The second stage weight loss of 4 % could be attributed to the removal of residual TEOS as well as structural water. In OT-Si-SPIONs initially 14.6 % weight loss was observed till 193.8 °C which is due to loss of moisture and volatile components. Further, from 194-424 °C weight loss of 11.9 % was there due to loss of structural water or entrapped hydroxyl groups on the surface of nanoparticles and also may be because of degradation of *oxytyramine*. After that, no significant loss was seen till 750 °C which showed better thermal stability of OT-Si-SPIONs. Also very less percentage of weight loss was observed at around 100 °C which confirms the stability of the catalyst in our reaction protocol.

View Article Online
DOI: 10.1039/C5RA20150K

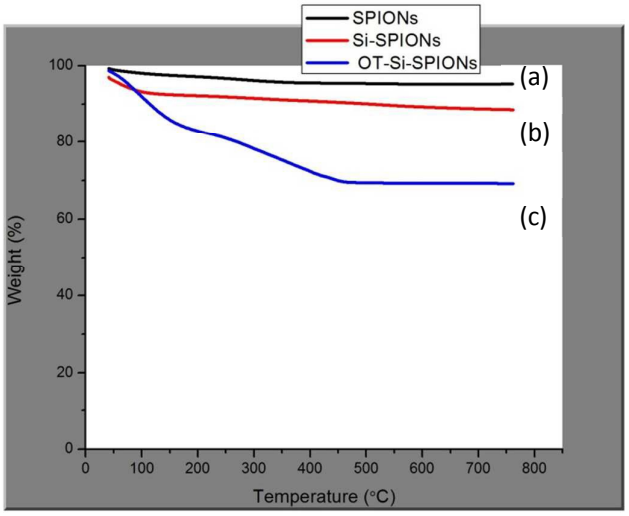

Fig. 6 TGA plots of: (a) SPIONs; (b) Si-SPIONs; (c) OT-Si-SPIONs.

2.3 Catalytic activity of OT-Si-SPIONs

The catalytic activity of OT-Si-SPIONs was tested as a heterogeneous catalyst (Scheme-II) under various conditions (Table 1) by chosing reaction of cyclohexanone (1), aniline (2a) and trimethylsilylcyanide (3) as a model reaction. Initially the influence of the catalyst on the model reaction was explored at room temperature by performing the reaction without catalyst and with catalyst (OT-Si-SPIONs) giving 67.59 % yield of the product in 94 minutes and 94.48.30 % yield of the product in 7 minutes respectively (Table 1, Entry 1, 2). These results encouraged us to optimize the reaction conditions. Hence further study of the loading of the catalyst was examined. As shown in Table 1, it was found that the catalyst loading affected the reaction obviously. The use of 2.5 mg of OT-Si-SPIONs catalyst gave 4a in only 81.72 % yield (Table 1, Entry 3). With 5 mg of the catalyst yield has been increased to 94.48 % taking time of 7 minutes to complete the reaction (Table 1, Entry 2). Further on increasing the amount of the catalyst, decrease in yield of 4a upto 86.43 % was obtained (Table 1, Entry 6). Thus 5 mg of the catalyst was the best choice.

In the subsequent study the reaction was conducted with various solvents to find out the appropriate solvent. Various solvents like H_2O, CH_3OH, C_2H_5OH, THF, Toluene, CH_3CN and H_2O: C_2H_5OH (1:1) mixture have been tried in the model reaction (Table 1, Entries 7-13). Among all of these solvents reaction with CH_3CN gave the best results with 83.43% yield in 18 minutes (Table 1, Entry 10). Further the model reaction was also carried out in the absence of solvent which gave the best yield of 4a i.e. 94.48 % in 7 minutes (Table 1, Entry 2).

The effect of temperature was studied by carrying out the model reaction at different reaction conditions under the optimized conditions (R.T., under refluxing on water bath [≈60°C], under refluxing on oil bath at 120°C) (Table 1, Entries 2, 14, 15) and the best results were obtained at R.T. (Table 1, Entry 2).

View Article Online
DOI: 10.1039/C5RA20150K

Using all the optimized reaction conditions, the model reaction was carried out to investigate the reaction time which was found to be 7 minutes at room temperature for compound 4a.

Further to examine the significance of supporting the catalyst and efficiency of protocol bare Fe_3O_4 nanoparticles (Table 1, Entry 16), silica coated Fe_3O_4 nanoparticles (Table 1, Entry 17), bulk oxytyramine (Table 1, Entry 18) were also studied. To our delight, the best results were obtained with our catalyst being reported in this paper. These results confirm that the catalytic activity derives from the oxytyramine species present on the nanocatalyst surface as well as it is increased significantly due to increase in the surface area of the catalyst , which is a result of supporting the active phase i.e. oxytyramine on nanosized material.

Table 1 Optimization of different proportions of OT-Si-SPIONs nanocatalyst along with solvents and temperature for the synthesis of 4a.

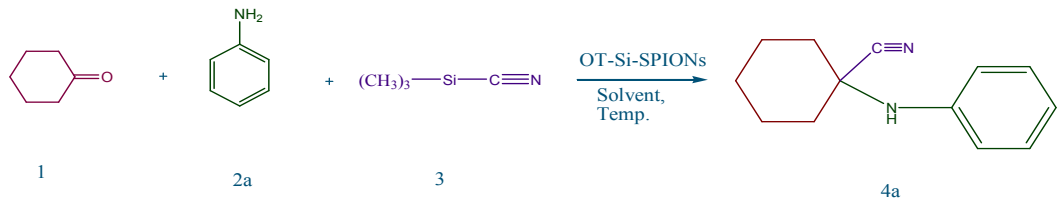

1 2a 3 4a

Scheme- II

Entry	Catalyst Amount (in mg)	Solvent	Temperature (°C)	Yield/ Time (%) / (min.)
1	-	-	R.T.	67.59 / 94
2	5[a]	-	R.T.	94.48 / 7
3	2.5[a]	-	R.T.	81.72 / -
4	7.5[a]	-	R.T.	91.62 / 18
5	10[a]	-	R.T.	87.26 / 4
6	15[a]	-	R.T.	86.43 / 10
7	5[a]	CH_3OH	R.T.	58.61 / 24
8	5[a]	C_2H_5OH	R.T.	74.31/ 23
9	5[a]	H_2O	R.T.	51.05 / -
10	5[a]	CH_3CN	R.T.	83.43 / 18
11	5[a]	THF	R.T.	77.83 / 21
12	5[a]	Toluene	R.T.	79.25 / 20
13	5[a]	1:1 (C_2H_5OH:H_2O)	R.T.	52.59 / -
14	5[a]	-	60°C	65.67 / 29

View Article Online
DOI: 10.1039/C5RA20150K

15	5[a]	-	120°C	60.58 / 28
16	5[b]	-	R.T.	79.94 / 1 day
17	5[c]	-	R.T.	82.19 / 1 day
18	5[d]	-	R.T.	76.05 / 28

Reaction conditions a: cyclohexanone (1, 1 mmol), aniline (2a, 1 mmol), Trimethylsilylcyanie (TMSCN, 3, 1.3 mmol), OT-Si-SPIONs (5 mg), b: Fe_3O_4 (SPIONs) as catalyst, c: Si-Fe_3O_4 (Si-SPIONs) as catalyst, d: Oxytyramine (OT) as bulk catalyst.

Further the versatility of this protocol was examined by the reaction of cyclohexanone and TMSCN with different amines under the optimized reaction conditions and the results are summarized in Table 2. Reactions were carried out using 1mmol of cyclohexanone, 1mmol amines, 1.3 mmol of TMSCN and low catalyst loading (5 mg) in solvent less condition. The reaction mixture was stirred using a magnetic stirring bar at room temperature. Various substituted amines like amines containing both electron donating as well as electron withdrawing groups (Table 2) have been investigated. Amines containing both electron withdrawing and electron donating groups showed almost similar trend of reactivity. The completion of the reaction was indicated by solidification of reaction medium and TLC. After completion, 5 ml of methanol was added to dissolve the product completely and catalyst was separated magnetically. Formation of no byproduct was observed. The product was then recrystallized with methanol and was characterized with melting point and ^{1}H-NMR spectroscopic techniques.

Table 2 OT-Si-SPIONs catalyzed reaction with different substituted amines to synthesize cyclohexanecarbonitriles

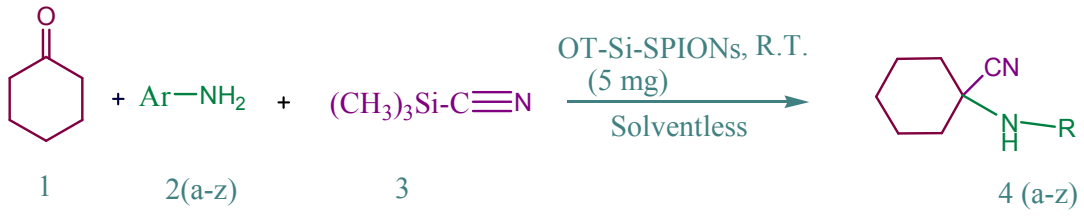

Entry	Ar (Amine)	Product	Time (min.)	Yield (%)
2a	C_6H_5	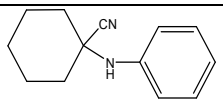 4a	7	94.48

View Article Online
DOI: 10.1039/C5RA20150K

2b	2-ClC_6H_4	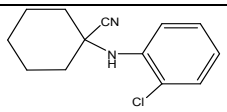 4b	17	48.33
2c	4-Cl C_6H_4	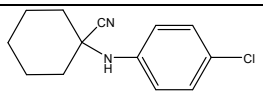 4c	23	97.44
2d	4-FC_6H_4	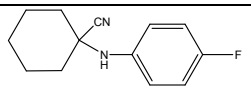 4d	4	94.60
2e	2-BrC_6H_4	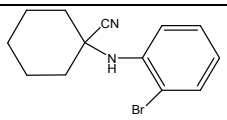 4e	12	45.50
2f	2-$OCH_3C_6H_4$	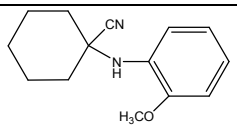 4f	66	52.69
2g	2-$CH_3C_6H_4$	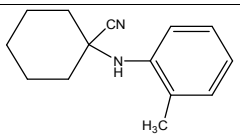 4g	45	78.96
2h	3-BrC_6H_4	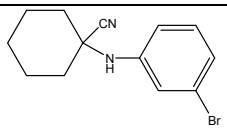 4h	11	89.76
2i	4-BrC_6H_4	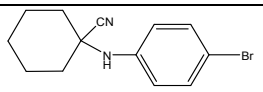 4i	7	91.60
2j	2-$OCH_2CH_3C_6H_4$	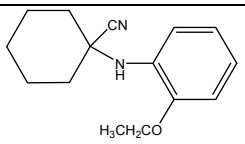 4j	62	29.82
2k	3-$CH_3C_6H_4$	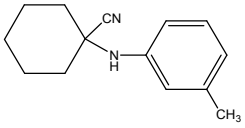 4k	42	92.06

View Article Online
DOI: 10.1039/C5RA20150K

2l	3-ClC_6H_4	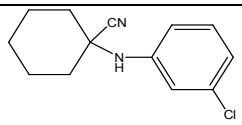 4l	16	54.29
2m	2-FC_6H_4	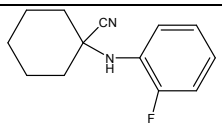 4m	19	68.24

Reaction conditions: Cyclohexanone (1, 1 mmol), amine (2a-z, 1 mmol), TMSCN (3, 1.3 mmol), OT-Si-SPIONs (5 mg)

The present protocol as compared to reported methods is more environmentally compatible, economical and green (Table 3).

Table 3 Comparison of synthesis of α-aminonitrile derivatives with reported protocols for compound 4a

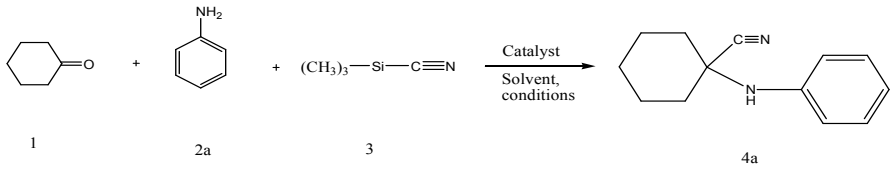

1 2a 3 4a

Entry	Catalyst used	Conditions/ Solvent	Catalyst loading	Time (min.)	Yield (%)
1.	B-MCM-41[48]	* R.T./ EtOH	50 mg	404	89
2.	MCM-41-SO_3H[49]	* R.T./ EtOH	5 mg	180	91
3.	SBA-15-Ph-Pr-SO_3H[50]	^50 °C/ -	5 mol%	480	95
4.	$LiBF_4$[51]	# R.T./ -	0.1 eq.	25	88
5.	Sulfated Tungstate	¤ R.T./ -	10 wt%	360	88
6.	OT-Si-SPIONs	$^{\Delta}$R.T./ -	5 mg	7	94.48 (Present work)

* For 1 mmol of 1, 1 mmol of 2a and 1.2 mmol of 3, ^ For 3 mmol of 1, 3 mmol of 2a and 3.6 mmol of 3, # For 1 eq of 1, 1 eq of 2a and 1.1 eq of 3, ¤ For 1 eq of 1, 1 eq of 2a and 1 eq of 3, $^{\Delta}$ For 1 mmol of 1, 1 mmol of 2a and 1.3 mmol of 3.

View Article Online
DOI: 10.1039/C5RA20150K

2.4 Recyclability of catalyst

The ability of the OT-Si-SPIONs particles to act as a heterogeneous recyclable catalyst has been examined by carrying out repeated runs on the same batch of the used 5 mg magnetic catalyst in reaction of cyclohexanone (1, 1 mmol), aniline (2a, 1 mmol) and TMSCN (3, 1.3 mmol) (Fig. 8). The catalyst was separated from the reaction mixture magnetically after the completion of the reaction and was washed with methanol and acetone successively and then was dried at 50º C for 30 minutes. The catalytic activity of the nanoparticles did not decreased significantly even after five catalytic cycles. The TEM analysis (Fig. 2d) of the used catalyst revealed that the morphology of the recovered nanoparticles remained almost unaltered.

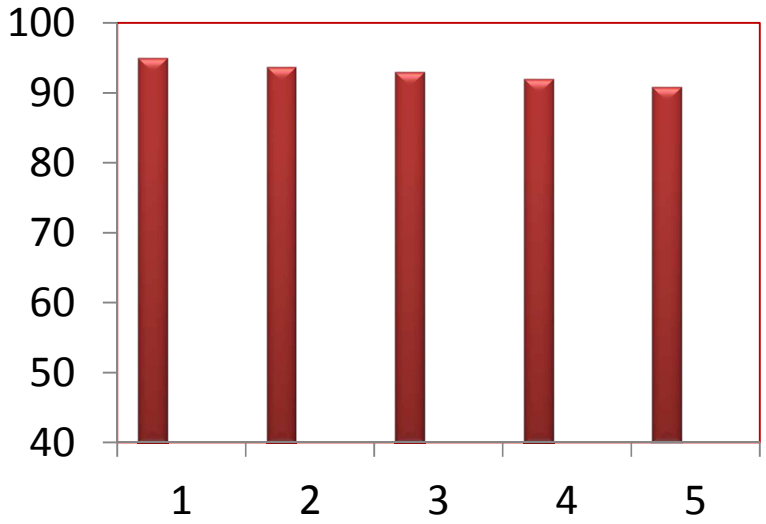

Figure 8 Recyclability of OT-Si-SPIONs upto 5 cycles

Scheme III represents the proposed mechanism for the synthesis of cyclohexanecarbonitriles. The catalytic NH_2 group forms H-bondng with the O of cyclohexanone thus facilitating the rate determining step of Strecker reaction i.e. formation of imine intermediate, which further reacts with TMSCN to form the product.

View Article Online
DOI: 10.1039/C5RA20150K

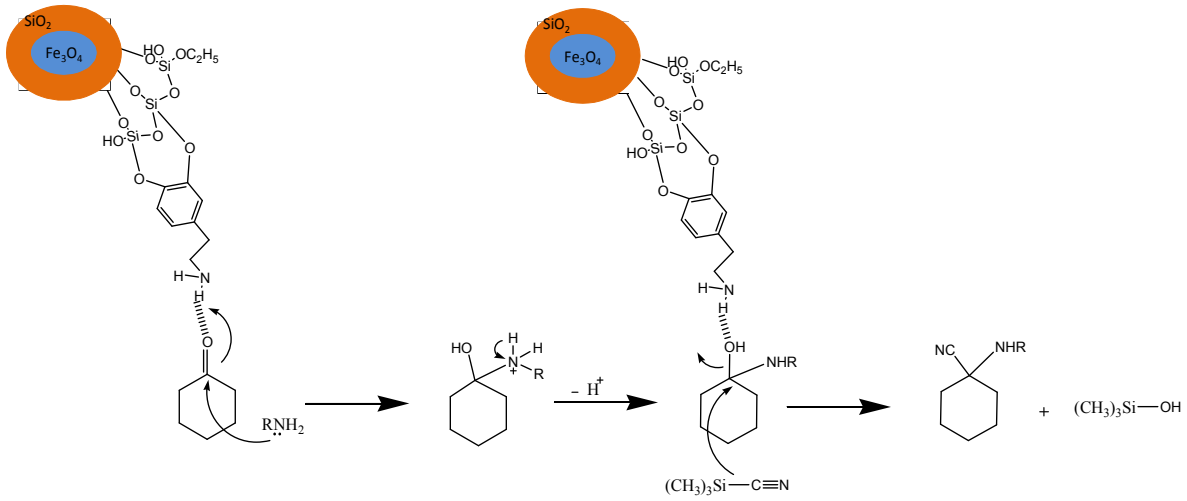

Scheme-III Proposed mechanism for synthesis of cyclohexanecarbonitriles

3. Experimental Section

3.1 Materials

All chemicals were purchased from local dealers and were used without any further purification.

3.2 Instrumentation

Fourier transform infrared spectra (FT-IR) were recorded using Perkin Elmer spectrum RX-I Fourier transform infrared spectrophotometer using KBr pellets in the scan range of 4000- 400 cm^{-1}. The crystalline phase of the nanoparticles was characterized by means of X-ray diffraction (XRD) measurements using Cu Kα radiation (λ=0.154 nm) on Panlytical XPERTPRO (NDP) X-ray diffractometer in the 2θ range of 15-80°. The morphology, nanostructure and particles size of the functionalized nanoparticles was studied by transmission electron microscopy (TEM) on Hitachi S7500 instrument. The sample was prepared by dispersing a small amount of solid nanoparticles in ethanol and then it was deposited over carbon coated Cu grids by dropcasting and followed by drying. Magnetic measurements were carried out of dried sample to evaluate magnetic properties of multifunctional nanoparticles at room temperature. For this Vibrating Sample Magnetometry was carried out on Princeton applied research model 155. Scanning electron microscope images were taken on JEOL JSM-6610LV instrument. The thermogravimetric analysis (TGA), differential thermal analysis (DTA) and differential thermal gravimetry (DTA) curves were recorded using an EXSTAR6000TG/DTA 6300 instrument at heating rate of 10 °C/min. under nitrogen atmosphere. The surface area, pore volume and pore diameter of nanoparticles was obtained by micromeritics ASAP 2010 model of accelerated surface area and porosimetry system. The UV spectra have been examined on Agilent Technologies Cary series UV-Vis spectrophotometer. The organic products were

View Article Online
DOI: 10.1039/C5RA20150K

characterized by ^{1}H nuclear magnetic resonance spectroscopy at 400 MHz with the aid of Advance 400 spectrophotometer using tetramethylsilane as the internal standard and DMSO-d^{6} solvent.

3.3 Synthesis of OT-Si-SPIONs

3.3.1 Synthesis of SPIONs (Fe_3O_4 nanoparticles)

Superparamagnetic iron oxide nanoparticles were synthesized by modified co-precipitation method without using any surfactants at room temperature in an ambient atmosphere. Ferrous sulphate ($FeSO_4.7H_2O$) and ferric sulphate ($Fe_2(SO_4)_3.nH_2O$) were used as iron salts in their respective stoichiometry ratio Fe^{2+}: Fe^{3+} = 1:2. At first, 10 ml of aqueous solutions of both iron salts [Fe^{2+}(7.19 mmol, 2.0 g)] and Fe^{3+}[(13.0 mmol, 5.2 g)] were made separately and ultrasonicated for 15 minutes at room temperature. Both the solutions were mixed and again ultrasonicated for 30 minutes. Then NH_4OH (25%) was added dropwise to the above mixed solution to reach pH value of approximately 10 along with sonication and constant stirring to attain homogeneous mixture. After complete addition, the mixture was stirred at 60 °C for 1 hour. The precipitates were isolated in the magnetic field and the supernatant was discarded by centrifugation (5000 rpm, 15 min.). Successive washings with deionized water were done to attain pH ≈ 7. Then the precipitates were dried in an oven at 50 °C for 24 hours.

3.3.2 Preparation of silica coated magnetite nanoparticles (Si-SPIONs)

Stöber method [41] with some alteration and combination of sonochemistry was used to prepare silica layer encapsulated SPIONs. 0.5 g of as prepared Fe_3O_4 nanoparticles were dispersed in 50 ml of deionized water by sonication for 30 minutes. Precipitates were isolated magnetically and redispersed in 25 ml of water and 90 ml of ethanol by sonication for 30 minutes. Solution was turned basic by adding 5 ml (25%) of ammonia solution. After thorough mixing by mechanical stirrer, 7ml of TEOS was added dropwise. Then, the mixture was stirred for 5.5 hours at room temperature. The as prepared nanoparticles were washed several times, magnetically separated, centrifuged (3500 rpm, 15 min.) and dried in an oven at 50 °C. These nanoparticles obtained were abbreviated as Si-SPIONs.

3.3.3 Functionalization of Si-SPIONs with *oxytyramine* (OT)

Si-SPIONs (0.1 g) were added in a mixture of 5 ml of water and 1 ml of ethanol and was sonicated for 30 minutes. Side by side 0.1g (mmol) *oxytyramine* solution in 2 ml of water was also sonicated for 30 minutes. Both the solutions were mixed, sonicated for 15 minutes and stirred overnight at 50 °C. Then the particles were washed with water, centrifuged (5000 rpm, 15 min.) and dried in an oven at 50 °C.

3.3.4 General procedure for the synthesis of cyclohexanecarbonitriles

To the mixture of cyclohexanone (1 mmol, 103.64µl), amine (1mmol) and TMSCN (1.3 mmol, 162 µl) into a round-bottom flask, OT-Si-SPIONs (5 mg) was added and stirred at room temperature for

View Article Online
DOI: 10.1039/C5RA20150K

the desired time. The reaction progress was followed by solidification of the product as well as thin layer chromatography (TLC) in 30% ethylacetate: hexane solution. After the completion of the reaction, the solid was dissolved completely in 5 ml of methanol and the catalyst was separated by an external magnet, washed with CH_3OH, CH_3COCH_3 and dried for further use. The product was recrystallized with methanol which was further characterized by its melting point and ^{1}H-NMR.

3.3.5 Spectral data for all compounds

4a: 1-(phenylamino)cyclohexanecarbonitrile

M.p. 71-72°C; ^{1}H-NMR (400 MHz, $CDCl_3$) • (ppm): 1.27-1.33 (m, 1H), 1.57-1.77 (m, 6H), 1.79-1.8 (m, 1H), 2.31-2.34 (t, 2H), 3.62 (s, 1H, NH), 6.88-6.92 (t, 3H), 7.22-7.26 (t, 2H).

4b: 1-(2-chlorophenylamino)cyclohexanecarbonitrile

M.p. 89°C; ^{1}H-NMR (400 MHz, $CDCl_3$) • (ppm): 1.37-1.42 (m, 1H), 1.68-1.78 (s, 7H), 2.37-2.39 (t, 2H), 4.38 (s, 1H, NH), 6.75-6.80 (m,1H), 7.19-7.21 (d, 2H), 7.29-7.31 (d, 1H).

4c: 1-(4-chlorophenylamino)cyclohexanecarbonitrile

M.p. 98-100°C; ^{1}H-NMR (400 MHz, $CDCl_3$) • (ppm): 1.23-1.36 (m, 1H), 1.68-1.81 (m, 7H), 2.28-2.32 (m, 2H), 3.63 (s, 1H, NH), 6.82-6.86 (m, 2H), 7.17-7.21 (m, 2H).

4d: 1-(4-fluorophenylamino)cyclohexanecarbonitrile

M.p. 104-106 °C; ^{1}H NMR (400MHz, $CDCl_3$) • (ppm): 1.26-1.35 (m, 1H), 1.58-1.74 (m, 6H), 1.78-1.81 (m, 1H), 2.21-2.27 (m, 2H), 3.48 (s, 1H, NH), 6.90-6.98 (m, 4H).

4e: 1-(2-bromophenylamino)cyclohexanecarbonitrile

M.p. 82-84 °C; ^{1}H-NMR (400 Hz, $CDCl_3$) • (ppm): 1.65-1.80 (m, 8H), 2.34-2.37 (t, 2H), 4.40 (s, 1H, NH), 6.69-6.73 (t, 1H), 7.10-7.26 (q, 2H), 7.46-7.48 (dd,1H).

4f: 1-(2-methoxyphenylamino)cyclohexanecarbonitrile

M.p. 82-84 ºC; ^{1}H-NMR (400 MHz, $CDCl_3$) • (ppm): 1.25-1.36 (m, 1H), 1.67-1.79 (m, 7H), 2.37-2.39 (t, 2H), 3.84 (s, 3H), 4.35 (bs, 1H, NH), 6.81-6.83 (q, 2H), 6.87-6.91 (m, 1H), 7.08-7.10 (dd, 1H).

4g: 1-(2-tolylphenylamino)cyclohexanecarbonitrile

M.p. 68-70 ºC; ^{1}H-NMR (400 MHz, $CDCl_3$) • (ppm): 1.33-1.38 (m, 1H), 1.69-1.79 (m, 7H), 2.17 (s, 3H), 2.37-2.40 (t, 2H), 3.49 (s, 1H, NH), 6.78-6.82 (t, 1H), 7.10-7.18 (m, 3H).

4h: 1-(3-bromophenylamino)cyclohexanecarbonitrile

View Article Online
DOI: 10.1039/C5RA20150K

M.p. 94-98 °C; ^{1}H NMR (400MHz, $CDCl_3$) • (ppm): 1.25-1.37 (m, 1H), 1.67-1.81 (m, 7H), 2.31-2.35 (t, 2H), 3.71 (s, 1H, NH), 6.82-6.85 (d, 1H), 6.90-7.01 (d, 2H), 7.0-7.11 (t, 1H).

4i: 1-(4-bromophenylamino)cyclohexanecarbonitrile

M.p. 116-120 °C; ^{1}H NMR (400MHz, $CDCl_3$) • (ppm): 1.29-1.35 (m, 1H), 1.64-1.81 (m, 7H), 2.29-2.33 (q, 2H), 3.65 (s, 1H, NH), 6.77-6.80 (m, 2H), 7.31-7.34 (m, 2H).

4j: 1-(2-ethoxyphenylamino)cyclohexanecarbonitrile

M.p. 92-94 °C; ^{1}H NMR (400MHz, $CDCl_3$) • (ppm): 1.34-1.36 (m, 1H), 1.40-1.44 (t, 3H), 1.67-1.77 (m, 7H), 2.35-2.38 (d, 2H), 4.04-4.09 (q, 2H), 4.40 (bs, 1H, NH), 6.77-6.82 (m, 2H), 6.86-6.9 (m, 1H), 7.09-7.11 (d, 1H).

4k: 1-(3-tolylphenylamino)cyclohexanecarbonitrile

M.p. 88-90 ºC; ^{1}H-NMR (400 MHz, $CDCl_3$) • (ppm): 1.28-1.36 (m, 1H), 1.56-1.72 (m, 6H), 1.76-1.80 (m, 1H), 2.30-2.34 (q, 5H), 3.56 (s, 1H, NH), 6.71-6.74 (d, 3H), 7.10-7.14 (t, 1H).

4l: 1-(3-chlorophenylamino)cyclohexanecarbonitrile

M.p. 80 ºC; ^{1}H-NMR (400 MHz, $CDCl_3$) • (ppm): 1.32 (s, 1H), 1.67 (s, 7H), 2.33 (s, 2H), 3.70 (s, 1H), 6.23-6.25 (t, 1H), 6.8 (s, 2H), 7.1 (s, 1H).

4m: 1-(2-fluorophenylamino)cyclohexanecarbonitrile

M.p. ºC; ^{1}H-NMR (400 Hz, $CDCl_3$) • (ppm): 1.64-1.78 (m, 8H), 2.31-2.34 (t, 2H), 4.19 (s, 1H, NH), 6.45-6.89 (t, 1H), 7.0-7.26 (q, 2H), 7.41-7.48 (dd,1H).

4. Conclusions

In summary, a new type of versatile and efficient heterogeneous magnetic nanocatalyst (OT-Si-SPIONs) has been developed using combined sonochemical and co-precipitation process, further this recyclable catalyst has been successfully applied in the synthesis of various new cyclohexanecarbonitriles. The reaction was carried out under stirring at room temperatures which gave excellent results and render this protocol economical. Synthesis of cyclohexanecarbonitriles is rarely discussed because of its slow reaction rate but in our protocol these have been synthesized efficiently. The simple procedure for the catalyst preparation, easy recovery of the catalyst and recyclability of the catalyst without any significant loss in its activity even after 5 cycles makes it an ideal catalytic system. The excellent features of this protocol are short reaction time, simple work up process, green synthesis, no column process and environmentally benign.

Acknowledgements

View Article Online
DOI: 10.1039/C5RA20150K

We are thankful to SAIF, Panjab University Chandigarh for FT-IR, TEM and ^{1}H-NMR, IIT Ropar for SEM and XRD, CSMCRI Bhavnagar for BET. Two of the authors (P.A. and H.S.) are thankful to MHRD, UGC and NIT Jalandhar for providing the research fellowship.

References

1. R. K. Sharma, Y. Monga, and A. Puri, *Catal. Commun.*, 2013, **35**, 110–114.

2. J. Sun, G. Yu, L. Liu, Z. Li, Q. Kan, Q. Huo, and J. Guan, *Catal. Sci. Technol.*, 2014, **4**, 1246.

3. E. Rafiee and S. Eavani, *J. Mol. Catal. A Chem.*, 2013, **373**, 30–37.

4. R. B. Nasir Baig and R. S. Varma, *Green Chem.*, 2013, **15**, 398.

5. A. Maleki, *Tetrahedron Lett.*, 2013, **54**, 2055–2059.

6. B. Sreedhar, a. S. Kumar, and P. S. Reddy, *Tetrahedron Lett.*, 2010, **51**, 1891–1895.

7. W. Wu, Q. He, and C. Jiang, *Nanoscale Res. Lett.*, 2008, **3**, 397–415.

8. C. Hui, C. Shen, J. Tian, L. Bao, H. Ding, C. Li, Y. Tian, X. Shi, and H.-J. Gao, *Nanoscale*, 2011, **3**, 701–5.

9. A.-H. Lu, E. L. Salabas, and F. Schüth, *Angew. Chem. Int. Ed. Engl.*, 2007, **46**, 1222–44.

10. B. D. Terris and T. Thomson, *J. Phys. D. Appl. Phys.*, 2005, **38**, R199–R222.

11. J. Safari and L. Javadian, *Comptes Rendus Chim.*, 2013, **16**, 1165–1171.

12. A. K. Gupta and M. Gupta, *Biomaterials*, 2005, **26**, 3995–4021.

13. C. Alexiou, W. Arnold, R. J. Klein, F. G. Parak, P. Hulin, C. Bergemann, W. Erhardt, S. Wagenpfeil, and A. S. Lübbe, *Cancer Res.* , 2000, **60** , 6641–6648.

14. S. Laurent, S. Dutz, U. O. Häfeli, and M. Mahmoudi, *Adv. Colloid Interface Sci.*, 2011, **166**, 8–23.

15. L. Li, W. Jiang, K. Luo, H. Song, F. Lan, Y. Wu, and Z. Gu, *Theranostics*, 2013, **3**, 595–615.

16. I. Koh and L. Josephson, *Sensors (Basel).*, 2009, **9**, 8130–45.

17. A. Strecker, *Ann. der Chemie und Pharm.*, 1850, **75**, 27–45.

18. B. Karimi, A. Maleki, D. Elhamifar, J. H. Clark, and A. J. Hunt, *Chem. Commun. (Camb).*, 2010, **46**, 6947–6949.

19. M. Hatano, Y. Hattori, Y. Furuya, and K. Ishihara, *Org. Lett.*, 2009, 2007–2010.

20. S. C. Pan and B. List, *Org. Lett.*, 2007, **9**, 1149–1151.

21. K. Iwanami, H. Seo, J. C. Choi, T. Sakakura, and H. Yasuda, *Tetrahedron*, 2010, **66**, 1898–1901.

View Article Online
DOI: 10.1039/C5RA20150K

22. N. U. H. Khan, S. Agrawal, R. I. Kureshy, S. H. R. Abdi, S. Singh, E. Suresh, and R. V. Jasra, *Tetrahedron Lett.*, 2008, **49**, 640–644.

23. J. Jarusiewiez, Y. Choe, K. S. Yoo, C. P. Park, and K. W. Jung, *J. Org. Chem.*, 2009, **74**, 2873–2876.

24. G.-W. Zhang, D.-H. Zheng, J. Nie, T. Wang, and J.-A. Ma, *Org. Biomol. Chem.*, 2010, **8**, 1399–1405.

25. B. Karmakar and J. Banerji, *Tetrahedron Lett.*, 2010, **51**, 2748–2750.

26. G. K. S. Prakash, T. Mathew, C. Panja, S. Alconcel, H. Vaghoo, C. Do, and G. a Olah, *Proc. Natl. Acad. Sci. U. S. A.*, 2007, **104**, 3703–3706.

27. P. Fontaine, A. Chiaroni, G. Masson, and J. Zhu, *Org. Lett.*, 2008, **10**, 1509–1512.

28. M. L. Kantam, J. Yadav, S. Laha, P. Srinivas, B. Sreedhar, F. Figueras, V. De Lyon, and L. Cedex, 2009, 4608–4611.

29. M. M. Mojtahedi, M. Saeed Abaee, and T. Alishiri, *Tetrahedron Lett.*, 2009, **50**, 2322–2325.

30. F. Cruz-Acosta, A. Santos-Expósito, P. de Armas, and F. García-Tellado, *Chem. Commun. (Camb).*, 2009, 6839–6841.

31. D. Bandyopadhyay, J. M. Velazquez, and B. K. Banik, *Org. Med. Chem. Lett.*, 2011, **1**, 11.

32. A. Heydari, S. Khaksar, and M. Tajbakhsh, *Tetrahedron Lett.*, 2009, **50**, 77–80.

33. C. R. Razafindrabe, S. Aubry, B. Bourdon, M. Andriantsiferana, S. Pellet-Rostaing, and M. Lemaire, *Tetrahedron*, 2010, **66**, 9061–9066.

34. A. Arasappan, S. Venkatraman, A. I. Padilla, W. Wu, T. Meng, Y. Jin, J. Wong, A. Prongay, V. Girijavallabhan, and F. George Njoroge, *Tetrahedron Lett.*, 2007, **48**, 6343–6347.

35. B. C. Das, J. Anguiano, and S. M. Mahalingam, *Tetrahedron Lett.*, 2009, **50**, 5670–5672.

36. J. P. Abell and H. Yamamoto, *J. Am. Chem. Soc.*, 2009, **131**, 15118–15119.

37. J. K. Rajput and G. Kaur, *Catal. Sci. Technol.*, 2014, **4**, 142.

38. G. Kaur, J. K. Rajput, P. Arora, and N. Devi, *Tetrahedron Lett.*, 2014, **55**, 1136–1140.

39. O. Arias-Carrión and E. Pŏppel, *Acta Neurobiol. Exp. (Wars).*, 2007, **67**, 481–8.

40. H. Iida, K. Takayanagi, T. Nakanishi, and T. Osaka, *J. Colloid Interface Sci.*, 2007, **314**, 274–80.

41. W. Stöber, A. Fink, and E. Bohn, *J. Colloid Interface Sci.*, 1968, **26**, 62–69.

42. K. K. Senapati, C. Borgohain, and P. Phukan, *J. Mol. Catal. A Chem.*, 2011, **339**, 24–31.

43. B. Karami, S. J. Hoseini, K. Eskandari, A. Ghasemi, and H. Nasrabadi, *Catal. Sci. Technol.*, 2012, **2**, 331.

View Article Online
DOI: 10.1039/C5RA20150K

44. X. Huang, G. Wang, M. Yang, W. Guo, and H. Gao, *Mater. Lett.*, 2011, **65**, 2887–2890.

45. G. F. Goya, T. S. Berquó, F. C. Fonseca, and M. P. Morales, *J. Appl. Phys.*, 2003, **94**, 3520.

46. G. Leofanti, M. Padovan, G. Tozzola, and B. Venturelli, *Catal. Today*, 1998, **41**, 207–219.

47. M. Khalfaoui, S. Knani, M. a. Hachicha, and A. B. Lamine, *J. Colloid Interface Sci.*, 2003, **263**, 350–356.

48. M. G. Dekamin, Z. Mokhtari, and Z. Karimi, *Sci. Iran.*, 2011, **18**, 1356–1364.

49. M. G. Dekamin and Z. Mokhtari, *Tetrahedron*, 2012, **68**, 922–930.

50. B. Karimi and D. Zareyee, *J. Mater. Chem.*, 2009, **19**, 8665.

51. U. V. Desai, S. D. Mitragotri, T. S. Thopate, D. M. Pore, and P. P. Wadgaonkar, *Monatshefte fur Chemie*, 2007, **138**, 759–762.